

Biosupramolecular Nanowires from Chlorophyll Dyes with Exceptional Charge-Transport Properties**

Sanchita Sengupta, Daniel Ebeling, Sameer Patwardhan, Xin Zhang, Hans von Berlepsch, Christoph Böttcher, Vladimir Stepanenko, Shinobu Uemura, Carsten Hentschel, Harald Fuchs, Ferdinand C. Grozema, Laurens D. A. Siebbeles, Alfred R. Holzwarth, Lifeng Chi,* and Frank Würthner*

A lot of pivotal functions in nature depend on the self-organization of π -conjugated molecules into highly ordered structures. A splendid example are chlorosomes of green sulfur and non-sulfur bacteria, which are known to exhibit the most efficient light-harvesting (LH) antennae systems in nature.^[1] Lacking a protein matrix, the chlorosomal LH system is based solely on specifically functionalized chlorin derivatives, that is, bacteriochlorophyll (BChl) *c*, *d*, and *e*, the self-assembly of which is directed by noncovalent interactions to give a light-harvesting organelle with outstanding exciton-transport characteristics.^[2] On the other hand, during the last decade, a remarkable number of functional-dye-based self-assembled supramolecular materials has been designed for exciton transport,^[3] artificial photosynthesis,^[4] sensing purposes,^[5] and supramolecular electronics.^[6–8] In the area of supramolecular electronics, one-dimensional π stacks have attracted considerable interest to elucidate charge-carrier-

transport properties,^[7d] particularly in columnar liquid-crystalline mesophases,^[7] although tubular arrangements^[8] offer more robust percolation pathways for directed exciton and charge transport, because trap sites can be bypassed by the carriers.

In the early 1990s, Holzwarth and Schaffner introduced a straightforward model for the bacteriochlorophyll dye organization in chlorosomal LH antennae systems of green bacteria.^[9] According to this model, self-assembly of BChl *c*, *d*, and *e* is driven by metal–ligand coordination, hydrogen bonding and π – π stacking to give a tubular architecture with a diameter of 5–6 nm composed of 22 circularly arranged BChl dye stacks. These rod elements are further packed together to give an organelle with about 12 nm height, 30 nm width, and 100 nm length, surrounded by a lipid monolayer.^[10] While unambiguous experimental evidence for a tubular dye arrangement was never obtained for chlorosomes or in-vivo self-assembled BChl dyes, and alternative lamellae and multilayer tubular models were introduced recently,^[11] some of us obtained very homogeneous isolated-nanorod structures^[12,13] with a diameter of about 6 nm as confirmed by AFM analysis from self-assembled semisynthetic BChl *c* derivatives in organic solvents, namely zinc chlorins (ZnChls) that are equipped with hydrophobic dendron wedges.^[14] However, as for their natural counterparts, no experimental evidence for a tubular architecture could be found for these semisynthetic chlorin dye assemblies. In this communication, we show that easily accessible semisynthetic derivatives of BChl *c* equipped with hydrophilic dendron wedges self-assemble in water into well-defined nanotubes with a diameter of 6 nm and a length up to several micrometers, and that these nanotubes exhibit exceptional conductivities of 0.48 Sm^{-1} and charge-carrier mobilities of $0.03 \text{ cm}^2 \text{ V}^{-1} \text{ s}^{-1}$.

Toward this goal, our efforts were devoted to the amphiphilic semisynthetic water-soluble BChl *c* derivative **1** (for chemical structure, see Figure 1, left). For this zinc chlorin, we observed bathochromically displaced J-type absorption bands^[13] (see Figure S1 in Supporting Information) that are reminiscent to those found for BChl aggregates in chlorosomes,^[1b,2a] and the formation of highly defined nanorods with uniform heights of 5–6 nm according to AFM analysis (Figure S2). A schematic model of the nanotube is depicted in Figure 1 (right).

In striking contrast to natural BChl *c* derivatives bearing one hydrophobic side chain (C12 to C18 esterifying alcohols,

[*] Dr. S. Sengupta,^[a] Dr. X. Zhang, Dr. V. Stepanenko, Dr. S. Uemura, Prof. Dr. F. Würthner

Universität Würzburg, Institut für Organische Chemie and Center for Nanosystems Chemistry
Am Hubland, 97074 Würzburg (Germany)
E-mail: wuerthner@chemie.uni-wuerzburg.de

Dr. D. Ebeling,^[a] C. Hentschel, Prof. Dr. H. Fuchs, Prof. Dr. L. F. Chi
Westfälische Wilhelms-Universität Münster, Physikalisches Institut
Wilhelm-Klemm-Str. 10, 48149 Münster (Germany)
and

Center for NanoTechnology (CeNTech)
Heisenbergstr. 11, 48149 Münster (Germany)
E-mail: chi@uni-muenster.de

Dr. S. Patwardhan, Dr. F. C. Grozema, Prof. Dr. L. D. A. Siebbeles
Delft University of Technology, Optoelectronic Materials Section,
Department of Chemical Engineering
Julianalaan 136, 2628 BL, Delft (The Netherlands)

Dr. H. von Berlepsch, Dr. C. Böttcher
Freie Universität Berlin, Forschungszentrum für
Elektronenmikroskopie, Institut für Chemie und Biochemie
Fabeckstr. 36a, 14195 Berlin (Germany)

Prof. Dr. A. R. Holzwarth
Max-Planck-Institut für Bioorganische Chemie
Stiftstr. 34-36, 45470 Mülheim an der Ruhr (Germany)

[†] These authors contributed equally to this work.

[**] Financial support by the Volkswagen foundation within the priority programme “Complex Materials: Cooperative Projects of the Natural, Engineering, and Biosciences” is gratefully acknowledged.



Supporting information for this article is available on the WWW under <http://dx.doi.org/10.1002/anie.201201961>.

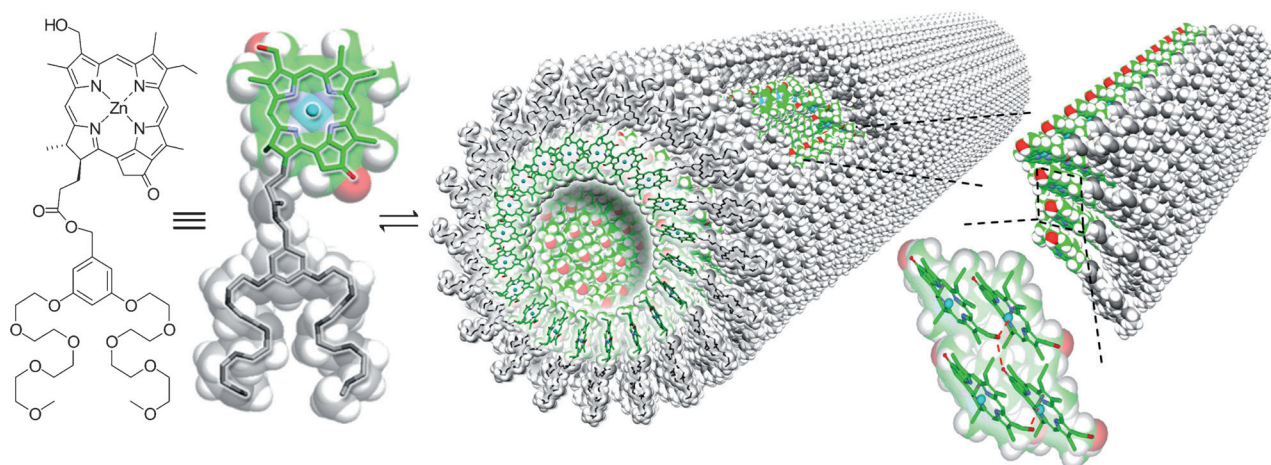


Figure 1. Chemical structure of zinc chlorin **1** and the corresponding space-filling (CPK) model (left). Schematic model of self-assembled nanotubes formed upon injection of a concentrated solution of chlorin **1** in methanol or THF into water (right).

for example, geranylgeraniol), solutions of amphiphilic zinc chlorin **1** aggregates remained stable against precipitation over several months in water/tetrahydrofuran (100:1; *v/v*) or water/methanol (100:1; *v/v*) mixture at concentrations of about 10^{-5} M as shown by UV/Vis (Figure S1) and dynamic light scattering (DLS) analysis (Figure S3 and S4). This stability is attributed to the dendron-wedge effect^[14] of the hydrophilic oligoethyleneglycol (OEG) chains in zinc chlorin **1**, which provide an ideal interface to the surrounding aqueous phase. Most importantly, after drop-casting an aggregate solution onto carbon-coated copper grid and negative staining with aqueous uranyl acetate, well-resolved individual nanotubes with diameters of approximately 6 nm and lengths of 300 nm up to 10 μ m could be observed by transmission electron microscopy (TEM) analysis (Figure 2a and Figure S5 and S6). Furthermore, beneath the isolated individual nanorods, a dense carpet of bundled nanorods is evident from the TEM micrograph that is obtained at this rather high concentration (Figure 2a).

Subsequent cryo-TEM studies on vitrified samples confirmed the presence of very stiff and elongated nanorods (> 100 nm) with a well-defined diameter (Figure 2b). Optimization of the imaging conditions (Figure 2c) afforded unambiguous proof of a tubular architecture that exhibits a higher contrast in the wall regions and a lower one in the interior. Figure 2d shows the overlaid line scans across seven arbitrarily chosen individual fibres (length of tubule segment \approx 100 nm) that show highly uniform aggregates. The density profiles indicate a typical tubular morphology, in which the total tube diameter amounts to (6.0 ± 0.5) nm, the tube wall maxima are 3.4 nm apart and the tubular wall has a thickness of about 2 nm, leaving a 2 nm central tube channel of lower density.

To the best of our knowledge, the well-defined structural homogeneity is unprecedented among artificial self-assembled tubular dye structures, and indicates the presence of highly stringent packing constraints in striking agreement with the tubular model proposed for natural chlorosomal LH systems (Figure 1, right).^[9] It appears that the increased

wedge size (two side chains in **1** instead of one side chain in natural BChl *c*, *d*, or *e*) and amphiphilicity imparted by the OEG chains are essential prerequisites to stabilize the arrangement of the chlorin dye stacks in a tubular architecture and to prohibit lamellar arrangements that are stabilized by interdigitation^[11b] of individual hydrophobic side chains.

Owing to their perfect shape, structural homogeneity and long-term stability in aqueous solution, these BChl-type nanotubes appear to be excellent candidates for supramolecular nanowires. So far, in contrast to the excellent exciton-transport characteristics,^[2,15] (bacterio-)chlorophyll dyes have not been demonstrated to possess outstanding charge-carrier-transport properties. Based on modest hole-carrier mobilities of 10^{-4} to 10^{-5} $\text{cm}^2 \text{V}^{-1} \text{s}^{-1}$ measured by time-of-flight measurements for microcrystalline chlorophyll *a* samples,^[16] Kassi et al. estimated an upper limit of $0.002 \text{ cm}^2 \text{V}^{-1} \text{s}^{-1}$ for an ideally ordered solid-state material of these dyes. Microwave-conductivity experiments on a liquid-crystalline zinc chlorin derivative performed by our research group showed charge mobilities exactly in this range.^[17]

In an identical experiment, the intrinsic charge-carrier mobility of zinc chlorin **1** in the solid state was characterized by the pulse-radiolysis time-resolved microwave conductivity (PR-TRMC) technique in the temperature range from -25 to 100°C (Figure S7 and Table S1). With this technique, a short pulse of high-energy electrons (10–50 ns, 3 MeV) generates a uniform concentration of charge carriers in the sample that is detected by a continuous source of microwaves. The first-order decay and long lifetime of the conductivity transients corroborate the perception of a one-dimensional hole-carrier transport within these tubular nanowires. With increasing temperature, the charge-carrier mobility is increased, thus indicating that the transport is thermally activated, which is typical for organic semiconductor materials.^[7] Most interestingly, the charge-carrier mobilities of approximately $0.03 \text{ cm}^2 \text{V}^{-1} \text{s}^{-1}$ are much higher than those of all previously investigated chlorophyll derivatives and even one order of magnitude higher than Kassi's estimated upper limit, highlighting the highly favorable π - π arrangement of BChl *c*

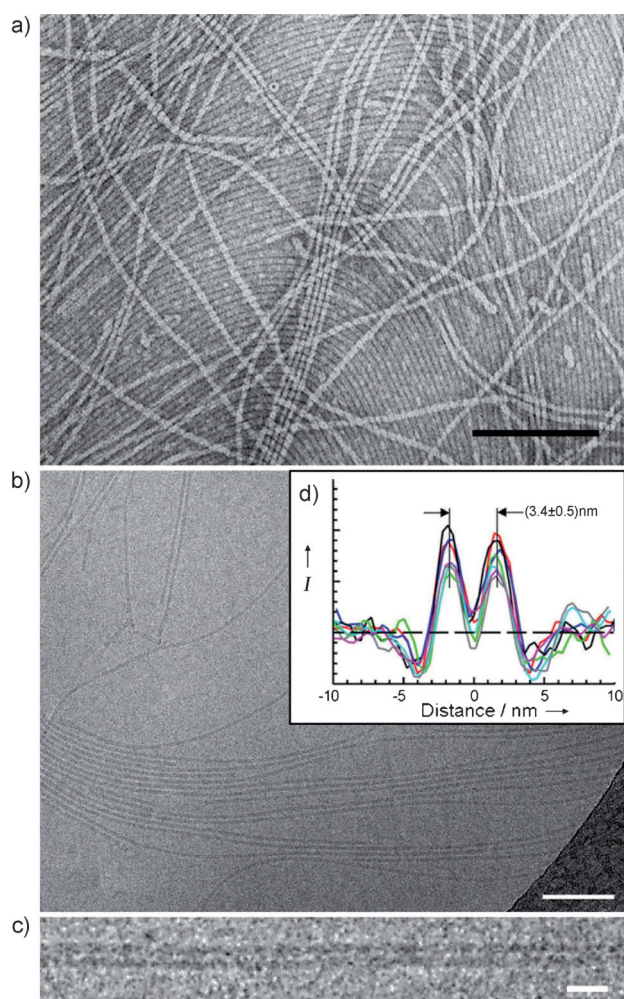


Figure 2. Transmission and cryo-transmission electron microscopy of chlorin nanotubes. a) TEM micrograph of **1** aggregates drop cast from water/methanol (100:1; $c \approx 10^{-5}$ M) and stained with 0.5% aqueous uranyl acetate at an accelerating voltage of 80 kV; scale bar is 100 nm. b) Cryo-TEM micrograph of a 5×10^{-6} M solution of chlorin **1** in water/methanol (100:1) showing fibrous aggregates embedded in vitrified ice. Scale bar: 100 nm. c) At high magnification, the tubular architecture of the fibrous aggregates becomes directly visible. Scale bar: 10 nm. d) Overlaid line scans across seven individual fibres (length of tubule segment ≈ 100 nm) show highly uniform aggregates.

derivatives not only for exciton but also for charge-carrier transport.

To monitor the transport of charges along individual nanowires, we applied the conductive AFM (C-AFM) method. This technique allows to monitor the pathways of electrical conduction between a metal-coated AFM tip and a conductive substrate and to relate it to the topography image that was recorded beforehand.^[18] To acquire information on the charge-carrier transport along macroscopic dimensions, we applied a special substrate to contact the chlorin nanowires. It consists of a non-conductive silicon oxide surface (Figure S8) and the conductive polymer poly(3,4-ethylenedioxythiophene):poly(4-styrenesulphonate) (PEDOT:PSS). A silicon oxide sample (Figure 3a, brown) was coated with a 10–15 nm thick layer of PEDOT:PSS

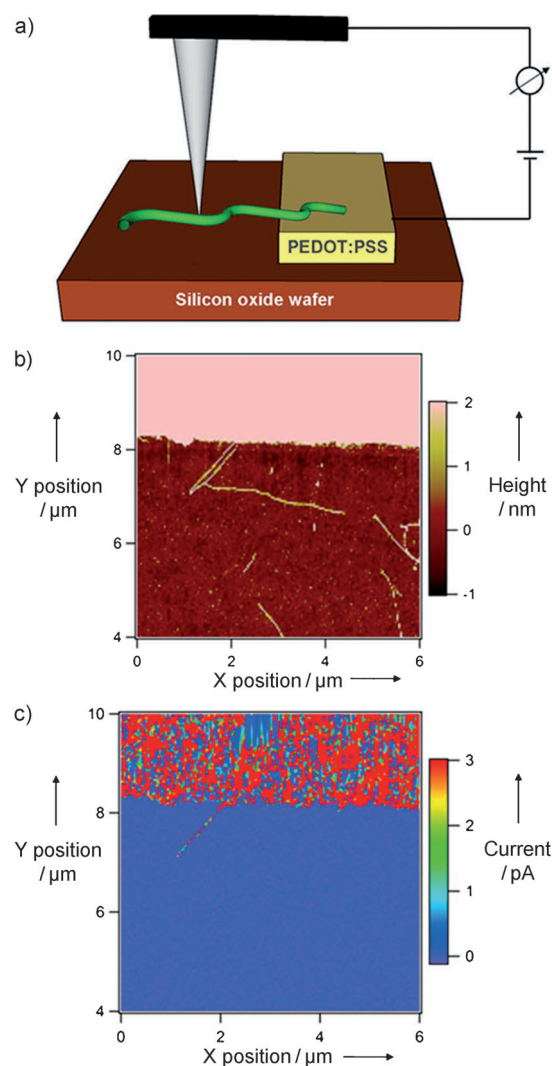


Figure 3. a) Schematic illustration of the C-AFM setup applied in this work. In C-AFM mode, a conductive cantilever (black/gray) is brought in contact with the nanowire (green). If attached to the conducting polymer (yellow) upon application of a voltage between tip and sample, a flowing current can be analyzed by an external electronic device. b) Topography image ($6 \times 6 \mu\text{m}^2$) of single chlorin nanowires adsorbed on a silicon oxide surface. c) Corresponding current image measured in the C-AFM mode.

(yellow). Subsequently, an AFM tip was employed to scratch $30 \times 30 \mu\text{m}^2$ squares into this polymer film to create adjacent conductive and isolating areas.^[19] Finally, the deposition of chlorin nanowires (green) was achieved by spin-coating. Figure 3b shows a typical topographical image of our samples.

The conductive polymer film appears in the top part of the image, while the scratched silicon surface with adsorbed nanowires is found in the bottom part. When a bias voltage is applied between the tip and the PEDOT:PSS contact, the corresponding current image is obtained (Figure 3c). The conductive polymer in the top part of the image exhibits a high conductivity in contrast to the silicon substrate (blue). Most interestingly, this image shows a single nanowire that is attached to the conductive polymer and shows a current signal. This is a clear evidence for the electrical conductivity

of chlorin nanowires. Notably, other nanowires that are not connected to PEDOT:PSS (Figure 3b) remain invisible in the C-AFM mode (Figure 3c).

To quantify the conductivity of these chlorin nanowires, we analyzed the current as a function of the distance to the PEDOT:PSS contact. Figure 4a shows a current image ($7.5 \times 10 \mu\text{m}^2$) of a single chlorin nanowire that is attached to a thin

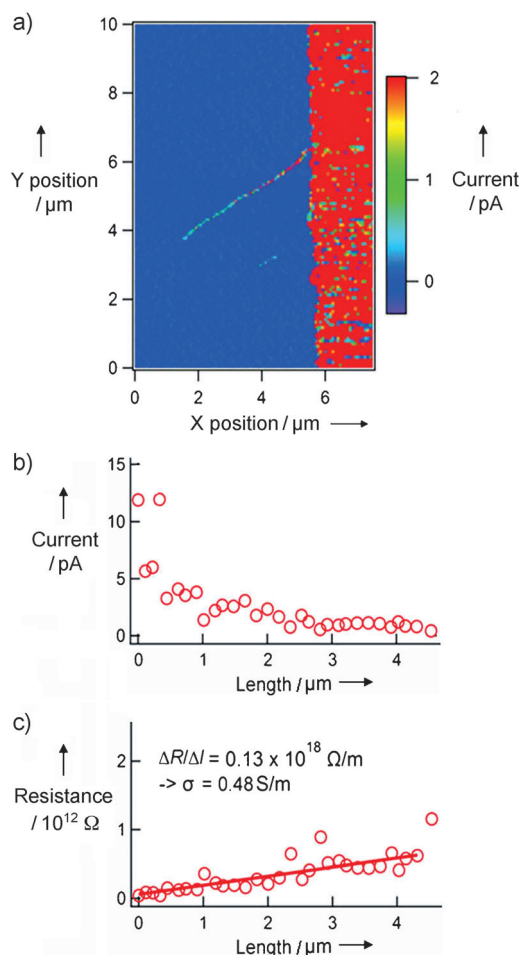


Figure 4. a) C-AFM image ($7.5 \times 10 \mu\text{m}^2$) of a nanowire that is electrically connected to the PEDOT:PSS conducting polymer on the right side. b) Measured current, and c) resistance of the nanowire as a function of its length.

film of conductive polymer. For this nanowire, a clear decrease of the conductivity can be recognized with increasing distance from the PEDOT:PSS contact by the color change from red to blue. In Figure 4b the measured current values are plotted versus the measured length of the nanowire. These values are used to calculate the local resistance R of the nanowire as a function of its length (Figure 4c). For this purpose, Ohm's law $R = U/I$ was used, in which U is the applied bias voltage and I is the measured current. To quantify the conductivity of these chlorin nanowires, we analyzed the current as a function of the distance to the PEDOT:PSS contact.

Assuming a three-dimensional conductor, the conductivity σ can be calculated from the slope of the $R(l)$ plot in

Figure 4c according to $\sigma = 1/(A \times \Delta R/\Delta l)$, in which A is the cross sectional area of the nanotube. For a 6 nm wide tube with an inner hollow of 2 nm, a conductivity of $(0.48 \pm 0.07) \text{ S m}^{-1}$ is obtained. We took care of keeping the loading force of the cantilever as low as possible. Nevertheless, values between 0.36 and 0.9 S m^{-1} for several chlorin nanowires were obtained with different C-AFM tips, while a large number of experiments failed because of a deformation or destruction of the wires that is attributed to the scanning movement of the AFM tip. Thus, although we kept the loading force of the cantilever as low and constant as possible during scanning, our conductivity values have to be considered as lower limits. In this regard it is particularly notable that these conductivity values are several orders of magnitude higher than those measured for other biomolecular structures, such as DNA.^[20]

In conclusion, we have shown that semisynthetic bacteriochlorophyll derivatives self-assemble into highly defined nanotubules reminiscent of the chlorosomal light-harvesting antennae of green bacteria. These nanotubules exhibit exceptional charge-transport properties. Indeed, conductive AFM measurements performed for single nanotubules showed conductivity values of approximately 0.48 S m^{-1} , which are unprecedented for natural supramolecular structures and are comparable in magnitude to those of semiconducting supramolecular oligomers and polymers. Thus, the prospects of tubular assemblies of semisynthetic chlorophyll derivatives for biosupramolecular electronics are apparent. Combining the excellent exciton-transport capabilities given by chlorosomal dye assemblies with semiconductivity, chlorophyll-dye-based bulk-heterojunction materials appear highly promising for organic photovoltaics.

Received: March 12, 2012

Published online: ■■■■■, ■■■■■

Keywords: biosupramolecular electronics · dyes/pigments · nanotubes · self-assembly · zinc chlorin

- [1] a) S. Ganapathy, G. T. Oostergetel, P. K. Wawrzyniak, M. Reus, A. G. M. Chew, F. Buda, E. J. Boekema, D. A. Bryant, A. R. Holzwarth, H. J. M. de Groot, *Proc. Natl. Acad. Sci. USA* **2009**, *106*, 8525–8530; b) T. S. Balaban, H. Tamiaki, A. R. Holzwarth, *Top. Curr. Chem.* **2005**, *258*, 1–38.
- [2] a) V. I. Prokhorenko, D. B. Steensgaard, A. R. Holzwarth, *Biophys. J.* **2000**, *79*, 2105–2120; b) G. D. Scholes, G. Rumbles, *Nat. Mater.* **2006**, *5*, 683–696.
- [3] H. Lin, R. Camacho, Y. Tian, T. E. Kaiser, F. Würthner, I. G. Scheblykin, *Nano Lett.* **2010**, *10*, 620–626.
- [4] a) M. R. Wasielewski, *Acc. Chem. Res.* **2009**, *42*, 1910–1921; b) S. Bhosale, A. L. Sisson, P. Talukdar, A. Fuerstenberg, N. Banerji, E. Vauthey, G. Bollot, J. Mareda, C. Röger, F. Würthner, N. Sakai, S. Matile, *Science* **2006**, *313*, 84–86.
- [5] a) S. W. Thomas III, G. D. Joly, T. M. Swager, *Chem. Rev.* **2007**, *107*, 1339–1386; b) P. Chithra, R. Varghese, K. Divya, A. Ajayaghosh, *Chem. Asian J.* **2008**, *3*, 1365–1373.
- [6] a) A. P. H. J. Schenning, E. W. Meijer, *Chem. Commun.* **2005**, 3245–3258; b) S. S. Babu, S. Prasanthkumar, A. Ajayaghosh, *Angew. Chem.* **2012**, *124*, 1800–1810; *Angew. Chem. Int. Ed.* **2012**, *51*, 1766–1776; c) D. González-Rodríguez, A. P. H. J. Schenning, *Chem. Mater.* **2011**, *23*, 310–325; d) E. Gomar-

- Nadal, J. Puigmartí-Luis, D. B. Amabilino, *Chem. Soc. Rev.* **2008**, 37, 490–504.
- [7] a) S. Sergeev, W. Pisula, Y. H. Geerts, *Chem. Soc. Rev.* **2007**, 36, 1902–1929; b) J. Wu, W. Pisula, K. Müllen, *Chem. Rev.* **2007**, 107, 718–747; c) S. Laschat, A. Baro, N. Steinke, F. Giesselmann, C. Hägele, G. Scalia, R. Judele, E. Kapatsina, S. Sauer, A. Schreivogel, M. Tosoni, *Angew. Chem.* **2007**, 119, 4916–4973; *Angew. Chem. Int. Ed.* **2007**, 46, 4832–4887; d) F. C. Grozema, L. D. A. Siebbeles, *Int. Rev. Phys. Chem.* **2008**, 27, 87–138.
- [8] J. P. Hill, W. S. Jin, A. Kosaka, T. Fukushima, H. Ichihara, T. Shimomura, K. Ito, T. Hashizume, N. Ishii, T. Aida, *Science* **2004**, 304, 1481–1483.
- [9] A. R. Holzwarth, K. Schaffner, *Photosynth. Res.* **1994**, 41, 225–233.
- [10] S. G. Sprague, L. A. Staehelin, M. J. Dibartolomeis, R. C. Fuller, *J. Bacteriol.* **1981**, 147, 1021–1031.
- [11] a) G. T. Oostergetel, M. Reus, A. G. M. Chew, D. A. Bryant, E. J. Boekema, A. R. Holzwarth, *FEBS Lett.* **2007**, 581, 5435–5439; b) J. Pšenčík, A. M. Collins, L. Liljeroos, M. Torkkeli, P. Laurinmaki, H. M. Ansink, T. P. Ikonen, R. E. Serimaa, R. E. Blankenship, R. Tuma, S. J. Butcher, *J. Bacteriol.* **2009**, 191, 6701–6708.
- [12] V. Huber, M. Katterle, M. Lysteska, F. Würthner, *Angew. Chem.* **2005**, 117, 3208–3212; *Angew. Chem. Int. Ed.* **2005**, 44, 3147–3151.
- [13] V. Huber, S. Sengupta, F. Würthner, *Chem. Eur. J.* **2008**, 14, 7791–7807.
- [14] B. M. Rosen, C. J. Wilson, D. A. Wilson, M. Peterca, M. R. Imam, V. Percec, *Chem. Rev.* **2009**, 109, 6275–6540.
- [15] G. S. Engel, T. R. Calhoun, E. L. Read, T. K. Ahn, T. Mancal, Y. C. Cheng, R. E. Blankenship, G. R. Fleming, *Nature* **2007**, 446, 782–786.
- [16] H. Kassi, R. M. Leblanc, S. Hotchandani, *Phys. Status Solidi B* **2000**, 220, 931–939.
- [17] S. Sengupta, S. Uemura, S. Patwardhan, V. Huber, F. C. Grozema, L. D. A. Siebbeles, U. Baumeister, F. Würthner, *Chem. Eur. J.* **2011**, 17, 5300–5310.
- [18] a) J. Puigmartí-Luis, V. Laukhin, Á. P. del Pino, J. Vidal-Gancedo, C. Rovira, E. Laukhina, D. B. Amabilino, *Angew. Chem.* **2007**, 119, 242–245; *Angew. Chem. Int. Ed.* **2007**, 46, 238–241; b) G. Bottari, D. Olea, C. Gómez-Navarro, F. Zamora, J. Gómez-Herrero, T. Torres, *Angew. Chem.* **2008**, 120, 2056–2061; *Angew. Chem. Int. Ed.* **2008**, 47, 2026–2031; c) S. Prasanthkumar, A. Gopal, A. Ajayaghosh, *J. Am. Chem. Soc.* **2010**, 132, 13206–13207.
- [19] L. Li, M. Hirtz, W. Wang, C. Du, H. Fuchs, L. Chi, *Adv. Mater.* **2010**, 22, 1374–1378.
- [20] D. Porath, A. Bezryadin, S. de Vries, C. Dekker, *Nature* **2000**, 403, 635–638.

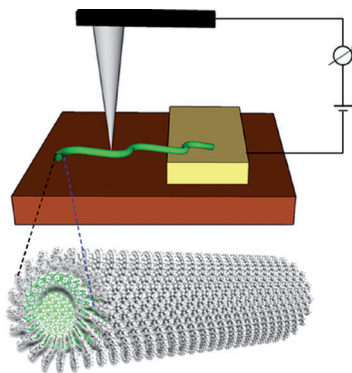
Communications



Nanotubes

S. Sengupta, D. Ebeling, S. Patwardhan,
X. Zhang, H. von Berlepsch, C. Böttcher,
V. Stepanenko, S. Uemura, C. Hentschel,
H. Fuchs, F. C. Grozema,
L. D. A. Siebbeles, A. R. Holzwarth,
L. F. Chi,* F. Würthner* — ■■■■—■■■■

Biosupramolecular Nanowires from
Chlorophyll Dyes with Exceptional
Charge-Transport Properties



Conductive tubes: Self-assembled nanotubes of a bacteriochlorophyll derivative are reminiscent of natural chlorosomal light-harvesting assemblies. After deposition on a substrate that consists of a non-conductive silicon oxide surface (see picture, brown) and contacting the chlorin nanowires to a conductive polymer (yellow), they show exceptional charge-transport properties.